Title: Macroevolutionary Constraint and Selection on Anti-Bat Moth Tails

Authors

Juliette J. Rubin[1,2*], Caitlin J. Campbell[2,3], Ana Paula S. Carvalho[1], Ryan A. St. Laurent[1,4], Gina I. Crespo,[1] Taylor L. Pierson[1], Robert P. Guralnick[5], Akito Y. Kawahara[1,2]

Affiliations

[1]McGuire Center for Lepidoptera and Biodiversity, Florida Museum of Natural History, Gainesville, FL, USA
[2]Department of Biology, University of Florida, Gainesville, FL, USA
[3]Bat Conservation International, Austin, TX, USA
[4]Department of Entomology, Smithsonian Institute, National Museum of Natural History, Washington, DC, USA
[5]Florida Museum of Natural History, University of Florida, Gainesville, FL, USA

*Now at: Smithsonian Tropical Research Institute, Gamboa, Panama

Corresponding author email: juliettejrubin@gmail.com

Keywords: Elaborate traits, predator-prey, Saturniidae, insectivorous bats, biogeography

Abstract

Elaborate traits evolve via intense selective pressure, often overpowering ecological constraints. Hindwing tails that thwart bat attack have repeatedly originated in moon moths (Saturniidae), with longer tails having more pronounced anti-predator effect. Understanding the relative evolutionary balance between predation pressure and possible limiting factors requires a macroevolutionary perspective. To estimate the eco-evolutionary forces shaping tails, we conducted phylogenetically-informed linear regressions. We built a well-sampled, time-calibrated phylogeny of the entirely tailed moth group (*Actias* + *Argema*) and performed ancestral state reconstruction and biogeographical analyses. To generate metrics of evolutionary pressures, we developed estimates of bat predator abundance and estimated environmental conditions associated with individual moth wing measurements. This integrative approach reveals evidence for positive selection on hindwing tails and body size by bats and negative selective pressure from environmental factors. Our study provides insight into the tradeoffs between strong biotic selective pressures and abiotic constraints that shape elaborate traits across the tree-of-life.

MAIN TEXT

1. Introduction

Elaborate traits provide a lens through which we can investigate opposing evolutionary pressures, as they are most likely to have emerged via strong selection. From the Narwal's tusk [1] to the peacock's train [2] to the porcupine's quills [3], elaborate traits often play a role in high-stakes inter or intraspecific interactions – either to win potential mates or to evade potential

predators. Due to their complex, conspicuous nature, these traits are commonly assumed to come with tradeoffs [4]. In some cases, tradeoffs have been empirically shown [5] but in many systems they can be hard to measure [6,7]. Frequently, when attempting to uncover tradeoffs, tests focus on short-term “acute trade-offs” (i.e., increased energy expenditure, reduced maneuverability, etc. [4]). It can be difficult to measure these acute costs, however, given that traits evolve as integrated components of an animal’s biology and thus commonly occur in tandem with cost-reducing characteristics [8]. As a result, longer-term tradeoffs are usually the more relevant constraining force on trait elaboration [4]. Here, we use macroevolutionary analyses to investigate the relative roles of biotic and abiotic drivers and constraints on the evolution of an elaborate wing trait in moths.

Moths in the family Saturniidae typically live for only a week as adults, during which time they do not feed and must locate mates at night to reproduce [9] while avoiding echolocating bats. At least five saturniid lineages have independently evolved hindwing tails with twisted and cupped ends [10]. Live bat-moth battles have revealed that these tails function as an anti-bat trait. Experimental alteration, as well as natural variation of tail length in the luna moth (*Actias luna*) and the African moon moth (*Argema mimosae*), showed that as tail length increases, moth escape success also increases [10,11]. Compared with individuals whose tails were removed, those with tails got away >25% more from bat attack, despite there being no measurable difference in moth flight kinematics between treatments [11]. Tails therefore represent a powerful countermeasure to a nearly ubiquitous nocturnal selective force [12] and their success is highlighted by their repeated convergence across the saturniid family tree [11].

Studies on alternative pressures of hindwing tails have thus far been unable to uncover another driver or acute trade-off. Mating trials using the luna moth have found no evidence that

tails are used in mate selection [13]. Experimental studies with tailed and non-tailed luna moth models and diurnally foraging birds indicated that tails do not increase roosting moth conspicuousness to these predators, nor do they protect the moth by breaking search image [14]. These wing appendages also do not seem to be either a hindrance or an asset to evasive flight maneuvers based on in-battle kinematic analysis [11].

Tails may instead be limited by longer-term tradeoffs. In general, Lepidoptera wings grow isometrically with body size and both attributes are influenced by nutrition [15,16]. The longer amount of time a lepidopteran can stay in its larval form acquiring resources, the larger its body and traits are likely to be. Developmental studies testing trade-offs between appendages in larval and pupal butterflies also indicate that growing and shaping wings has resource allocation costs [17,18]. An evo-devo study with the sphingid moth (the sister family to saturniids [19,20]) *Manduca sexta* showed that an increase in body size comes with a compensatory increase in development time or growth rate for wings to achieve appropriate scaling [21]. Thus, seasonality is expected to lead to a broad pattern where adult lepidopteran body size and associated traits are smaller in more seasonally variable environments (generally higher latitude regions) and larger in more consistent (lower latitude) environments with longer growing seasons [22–26]. Insects therefore do not seem to conform to the same ecogeographic laws that has been ascribed to endotherms. That is, body size does not necessarily increase at higher latitudes (Bergmann's Law) [24,27,28], nor do appendages (wings) appear to shorten at higher latitudes (Allen's Law) [29]. Instead, body size and wing lengths are likely governed by other physiological forces. In the case of elaborate wing structures, it may be that the energetics of building extra wing material for a tail is a limiting factor for moths living in more seasonally variable environments with shorter growing seasons.

To test the macroevolutionary pressures that have shaped the elaborate hindwing tail trait, we focused our analyses to an entirely tailed clade of Saturniidae: *Actias* + *Argema*. This group is primarily distributed across Asia, from present-day Russia to Indonesia, and Africa [30], thus covering a broad range of habitat with many environmental conditions and exhibiting an array of hindwing tail lengths. We hypothesized that across their distribution and evolutionary history, large insectivorous bats have exerted a positive selective force on saturniid hindwing tails, but that elongation has been constrained by abiotic environmental factors. We further hypothesized that the association between bat predation pressure and moth body size has not been as strong as the association between bats and hindwing tail length, but that body size has been equally susceptible to environmental constraints.

To test these hypotheses, we first built a well-sampled, time-calibrated phylogeny of the tailed moon moth clade (*Actias* + allies) and used this tree to trace the evolution of hindwing tails (Fig. 1). In order to access the hundreds of available records, we employed a novel trait measurement approach where we extracted wing lengths from digital images from museum collections and citizen science photos on iNaturalist, using the moth's antenna as a substitute scale bar, and verified this method using scaled images from museums. To parse hindwing length trends from changes in overall size, we used moth forewing length as a measure for body size [31,32]. We then investigated the effect of bat predation pressure (Fig. 2) and environmental factors (mean annual temperature, average seasonal temperature variation, length of growing season, average annual precipitation, and latitude) on these relative wing lengths using phylogenetically-informed regressions (Fig. 3). We estimated predation pressure on these moths by inferring the abundance of candidate bat predators (i.e., the number of individual bats of sufficiently large insectivorous species) in regions overlapping our focal moth species (Fig. 2).

We predicted that in general, moth species whose distributions overlapped areas with greater insectivorous bat predation pressure would have longer tails than species inhabiting less bat-rich areas. We also predicted that this trend would be curtailed in regions with high seasonal temperature variability. While we expected body size to follow similar patterns, we predicted the relationship between bat predation and size would be less pronounced. Using a macroevolutionary approach, we therefore aim to elucidate the environmental and biological pressures driving trait elaboration in moths.

2. Materials and methods

(a) Taxon sampling and DNA extraction

To reconstruct a well-sampled phylogeny of *Actias*, we used a combination of data previously published (6 ingroup species) [11] and newly sampled specimens from the McGuire Center of Lepidoptera and Biodiversity at the Florida Museum of Natural History (MGCL), Gainesville FL, USA (MGCL) (14 ingroup species; see Dataset S1 on Dryad for more details). We extracted DNA from both frozen, papered specimens (i.e., stored in an envelope in a -80 freezer since collection) and dried, pinned specimens (i.e., traditional museum preservation method) using an OmniPrep Genomic DNA Extraction Kit (G-Biosciences, St. Louis, MO) and evaluated DNA quality using agarose gel electrophoresis and quantity using Qubit 2.0 fluorometer (ThermoFisher Scientific). We sent our extracts to RAPiD Genomics (Gainesville, FL, USA) for library preparation, hybridization enrichment and sequencing using an Illumina HiSeq 2500 (PE100).

We analyzed our dataset using the Anchored Hybrid Enrichment (AHE) pipeline of Breinholt et al. [33]. We direct readers to this paper for detailed methods, but in brief, this pipeline uses an iterative probe-baited assembly process to clean raw reads and return an aligned set of orthologs for each locus in the probe kit. Because saturniids are in the superfamily Bombycoidea, we used the Bom1 probe kit (895 total loci) with *Bombyx mori* as our reference taxon [19]. We focused our analyses to coding regions (exons) and used MAFFT to align our sequences. We removed all loci that had <50% taxon coverage (40%), leading to a total data set of 535 loci. To ensure that each locus was in the correct frame and did not contain any spurious nucleotides, we visualized each file in AliView [34] and made any necessary manual edits. To assemble our supermatrices, we used FASconCAT-G v1.02 [35]. Cleaned probe regions and supermatrices can be found on Dryad (www.datadryad.org/xxxx).

(b) Phylogeny and estimation of divergence times

We reconstructed phylogenies with maximum likelihood (ML) and Bayesian inference (BI) optimality criteria, in IQ-TREE [36] and BEAST [37], respectively (Figs. S1-3). We built our maximum likelihood tree using IQ-TREE with the following commands: for one tree we used the 'MFP+MERGE' model, which maximizes model fit by sequentially merging pairs of genes (Fig. S1). For best compatibility with BEAST, we also built an ML tree using '-m TESTMERGE', which operates similarly to ParitionFinder [38], and then specified only BEAST-applicable models: JC69, TN93, K80, F81, HKY, SYM, TIM, TVM, TVMef, GTR. For both ML trees, we calculated support values using 1000 ultrafast bootstrap replicates via '-bb 1000' and 1000 Shimodaira-Hasegawa approximate likelihood ratio test replicates via '-alrt

1000'. We used the '-bnni' command, which protects against overestimating branch supports by employing a hill-climbing nearest neighbor interchange (NNI) technique [36] (Fig. S2). We also performed a multispecies coalescent analysis with ASTRAL, which estimates gene trees individually and then finds a summary species tree [39] (Fig. S4). This tree did not conflict significantly with our ML tree and we focus our analyses to the ML and Bayesian trees.

To generate our BEAST trees, we used BEAUTI v.1.8.4 [37] to create our command file. To infer divergence times, we used four secondary calibration points from Kawahara et al. [20]: Lasiocampoidea/Bombycoidea + other leps (78.61 – 99.27 mya), Lasiocampoidea + Bombycoidea (74.15 – 94.4 mya), Sphinigdae + Saturniidae (56.86 – 75.42 mya), Saturniidae (33.82 – 51.24), Saturniini (14.54 – 30.63). We used uniform distributions as calibration priors and an uncorrelated relaxed clock model. We used our phylogeny inferred by IQ-TREE as the starting tree (Fig. S1), with calibration nodes manually set within the bounds of their age ranges using Mesquite [40]. We built Bayesian trees with either a fixed tree topology, to constrain the tree to the topology of the maximum likelihood input, or a classic operator mix, to allow BEAST to infer topology. We ran separate trees using both Yule process and Birth-Death tree priors, with the Markov Chain Monte Carlo (MCMC) set to 200 million generations, sampling every 20000 trees to calculate posterior probabilities. We used the 'path sampling/stepping-stone sampling' function to enable comparison of the log marginal likelihood across trees that varied by tree priors and operator mix. Based on these comparisons, we decided to use the Bayesian fixed tree with a Birth-Death model for all further analyses (Fig. S3). All analyses were performed on the University of Florida's high-performance computing cluster, HiperGator2.

(c) Ancestral range estimation

To estimate ancestral ranges, we used the R package BioGeoBEARS [41] (BGB) to fit a dispersal-extinction-cladogenesis (DEC) model. We used our BEAST maximum clade credibility tree and pruned outgroups to focus solely on species of interest and a few most closely related sister taxa. Due to the young age of this clade, we did not add time stratification layers. We gathered general extant distributions of tailed moon moth species from GBIF and iNaturalist occurrence records (Research Grade only). Following classic biogeographical subdivisions of land areas based on ocean and mountain barriers, we defined the following seven regions: Africa (F), Americas (A), Europe (E), Philippines (H), Indomalaya + Greater Sunda Islands (M), Palearctic (P), and Wallacea (W) (Fig. S5). To limit permutations and in keeping with extant ranges, we limited our possible range outcomes to a maximum of 2 and defined the combination of regions that were possible (i.e., adjacent regions). We built a dispersal multipliers matrix following Toussaint et al. [42] and an extant regions matrix from GBIF, iNaturalist and museum collection locality data, as well as expert input (Stefan Naumann and R.A.S.; see Supplementary Archive 4 on Dryad).

(d) Bat predation pressure

We generated species distribution models (SDMs) for bats carefully selected to represent likely saturniid predators. Our selection process identified bats that are primarily insectivorous and of sufficient size to be common predators that would exert strong evolutionary pressure on the moths, avoiding those that might occasionally pursue insect prey under limited circumstances (e.g., frugivores that may opportunistically prey upon insects, such as Phyllostomids [43]). We

first identified all bat families where more than ≥ 50% of genera are aerial insectivores. From these families we selected genera where ≥ 50% of species are large (≥10g on average) aerial insectivores, and finally filtered the data set to just species that also followed this description (Dataset S2). We chose this size threshold based on observations of bat behavior in the lab [10,11] and the general scaling of bat size to size of prey items [44]. After filtering, 179 species (59% of our initial target list) had sufficient occurrence records to reliably fit SDMs (Fig. 2).

We leveraged an SDM-generation pipeline optimized for generating the distribution models of hundreds of species [45,46], customized to enhance performance for bats. First, we retrieved all bat occurrence records from the Global Biodiversity Information Facility (https://www.gbif.org/) and iDigBio (https://www.idigbio.org). We harmonized the taxonomy of records to the target species list using species definitions and synonyms from [47]. This matching was done using a manually-generated synonyms list for each targeted species. Data were cleaned with the "CoordinateCleaner" R package [48] and vetted with two rounds of manual checks. For each species with occurrence records, we defined accessible area using a dynamic alpha hull encompassing cleaned points and buffered by 200 km. Dynamic spatial thinning was conducted on points as in [46], with the total accessible area determining the degree and rigor of thinning; model outputs were further tuned with manual checks to remove additional spatial biases.

We selected model predictors based on other macroecological studies of bats [49–52]; for example, we used topological ruggedness and roughness as proxies for cave and carst roosting habitats used by bat species [49]. Initial models were fit using 15 candidate predictors from BioClim (BIO1–2,4–6,12–17 [53]), three topographic (elevation, roughness, and terrain roughness index [54]), and one from MODIS data (percent tree cover [55]). The initial candidate

predictors were selected to reduce collinearity while representing biologically plausible factors related to bat ecology. We further reduced model collinearity by iteratively refitting MAXENT models using default settings until all variance inflation factors were below 5. Using species-specific selected predictors, we quantitatively evaluated a suite of Maxent models with different tuning parameters to minimize model complexity and prevent overfitting using the R package ENMeval [56], using possible tuning parameters described in [46]. Final models were subject to an additional round of manual checks and adjusted or discarded if excessive commission or omission were apparent. We estimated species richness as the summed clog-log probability values from continuous surfaces, as recommended in [57]. To generate our estimates of bat abundance, we multiplied the clog-log probability SDM surface for each species by the population estimates provided in [58] and then divided by the sum of the clog-log surface to estimate the number of individual bats of a species in each 4664 m x 4664 m grid cell. Population estimates were generated via a regression model that incorporates average body mass (log transformed and z-score normalized) and IUCN Red List category for the species [58]. We then summed each species-specific density surface to estimate total bat density at each relevant location, and finally report the bat density surface in areas that overlap the moth species of interest (Fig. 2). For both bat richness and abundance, we extracted values at each site associated with moth hindwing length measurements. Code used to generate bat SDMs can be found at: zenodo.org.

(e) Hindwing tail trait acquisition

To extract wing measurements and associate these measurements with the individual's coordinates, we gathered photographs from both natural history collections, including MGCL,

American Museum of Natural History (AMNH), New York, NY, USA, and Stefan Naumann's collection, (Berlin, DE), and publicly sourced data repositories, including GBIF and iNaturalist (see Dryad for all photos). To scrape images and associated coordinates from these online repositories, we used the function *occ_cite* in the package "rgbif" [59] (see script on Dryad). While iNaturalist vastly increased our number of observations per species over museum specimens alone, photos on this site are unstandardized and most often are not associated with a scale bar. We therefore sought to find an alternative means of extracting a measurement of tail length. We determined that the most commonly visible components of the moth in these pictures were the forewings, hindwings, and antennae. Moreover, antennae length had a low correlation with HW, FW, and body length in these species (Fig. S6). We therefore used the antennae of each animal as a standard by which to measure hindwing length. To verify that HW length/antennae length would lead to similar relative measurements in both scaled (museum) and unscaled (iNaturalist) photos, we took length measurements from museum photos in imageJ [60], first scaling using the scale bar in the photo, and next without using the scale bar. Using the "Segmented line" tool in imageJ, we measured antennae length from tip to junction with head and using the "Straight line" tool we measured hindwing length from tip of the tail to junction with thorax and forewing length from tip of the forewing to junction with thorax. We performed individual t-tests to ensure there were no significant differences between the relative hindwing lengths in scaled and unscaled photos (Table S2). We used only male moths for all analyses, as they are better represented in collections and citizen scientist repositories and likely face higher bat predation due to flying more to locate females [61]. We also made sure all measurements taken from all publicly sourced images were of high-quality, and of relatively un-damaged

specimens where the camera was at a perpendicular angle to the animal, to prevent inaccurate measurements due to distortion.

(f) Phylogenetically-informed trait analysis and ancestral state reconstruction

To determine the strength of biotic and abiotic pressures on relative hindwing length, we used the package "phyr", a mixed model approach to estimate evolutionary phenomena, accounting for phylogeny and spatial correlation [62]. We used relative hindwing length (log(HW length/Antenna length)) as our response variable and bat abundance, mean annual temperature, seasonality (standard deviation of mean annual temperature), average annual precipitation, and length of growing season as predictor variables. The phylogenetic covariation matrix and moth species were set as random effects. We took environmental variables from the WorldClim website, which averages values between the years 1970-2000. Temperature parameters are reported in °C * 10 and precipitation is in mm (https://www.worldclim.org/data/bioclim.html). We extracted length of growing period (LGP) values from The Food and Agriculture Organization Food Insecurity, Poverty and Environment Global GIS Database (UN FAO FGGD) [63] using ArcGIS and found the median of each LGP range. To ensure that variables were not multicollinear (vif < 3 [64]), we used the *vif* function from the package "car". All variables were mean center scaled using the function "scale" to make them comparable across highly varying units of measurement. We ran a series of models with single or multiple predictors and used their R^2 values, as well as a DIC scores from the pglmm regression, to determine best fit (Fig. 3; and see code and outputs in Dryad).

We conducted comparative trait analyses and ancestral state reconstruction using the *ContMap* function and estimated phylogenetic signal using the *phylosig* function in the

"Phytools" package [65]. While we used only scaled museum specimens for this analysis, we generated the same metric that we used for ecological models to maintain consistency: log(HW length/Antenna length). For comparative trait analyses using absolute hindwing length and absolute forewing length, see Figs. S7-8. To determine whether the best-fitting evolutionary parameter underlying this trait evolution was Brownian motion (BM; random walk), Ornstein-Uhlenbeck (OU; adaptive peaks), or early burst (EB; rapid then slow morphological evolution), we used the "Rphylopars" package [66]. We used SURFACE [67] to test for convergent trait regimes across the phylogeny (Fig. S9, and see code and outputs on Dryad).

3. Results

Using species observations from iNaturalist and museum collections, the best-sampled *Actias* phylogeny to date (Fig. 1), and a comprehensive set of species distribution maps (SDMs) for 179 insectivorous bat species (Fig. 2), we investigated the relationship between hindwing tail length and biotic and abiotic drivers. As with other phylogenetic studies of Saturniidae (e.g., 10, 11), we recovered a well-supported monophyletic group comprising *Argema* (*Actias* + *Graellsia*), sister to the Australian/Papua New Guinea clade *Syntherata* (*Opodiphthera* + *Neodiphthera*) (Fig. 1). While *Graellsia* has been known to be nested within *Actias* [68], and this was confirmed in our study, we maintain the convention of using the *Graellsia isabellae* nomenclature. Within the *Actias* + allies ingroup, our tree largely agreed with the typology of these previous, less densely sampled AHE trees, as well as a study that reconstructed a phylogeny based on 16 *Actias* + allies species based on molecules, morphology, and behavior [69].

We found that Brownian Motion was the best fitting evolutionary model underlying the hindwing trait. That is, the evolution of tail length can be best described by a random walk, in comparison to a model with adaptive peaks or an early burst model (see scripts in Dryad). In line with this result, we found significant phylogenetic signal in hindwing length (Pagel's lambda = 0.0003) and our SURFACE analysis [67] revealed only one hindwing length regime shift at the stem of *Argema* + *Actias* from the non-tailed sister taxa (Fig. S9). While we did not detect a signal of adaptive peaks in our dataset, our ancestral state reconstruction (ASR) analyses indicate that tails have repeatedly elongated in at least four separate lineages: *Argema mittrei* + *A. mimosae*, *Actias dubernardi* + *A. chapae*, *Actias rhodopneuma*, and *Actias maenas* + *A. philippinica* + *A. isis*. In only one case do we find evidence of tail length shortening (*Graellsia isabellae*) (Fig. 1).

To examine whether biogeographical history could explain some of the variation in hindwing tail length, we used BioGeoBEARS [41] to estimate ancestral ranges. We inferred a 0.99 probability that Africa is part of the ancestral range of the tailed moon moths (including *Argema* and *Actias* species). We also found a 0.99 probability that the Palearctic was part of the ancestral range of the *Actias* clade, which likely diversified ~10 mya within the Palearctic, with a later dispersal of *Actias* species to the Indo-Malaysian region by ~7 mya. It appears that a second wave of *Actias* moved into this region by about 3 mya, with a subsequent move to Wallacea and the rest of the Indo-Australian archipelago (Fig.1). It is unclear how *Actias* arrived in the Philippines, as there is a roughly equal likelihood that they colonized this region via Wallacea or from the Indomalaya region. We also do not have strong inference as to the exact manner in which *Actias* colonized Northern America and Europe, but our analysis indicates that they did so from the Palearctic region (Figs. 1, S5).

Our global phylogenetically-controlled linear regression model (pglmm) revealed that hindwing length exhibits a positive relationship with bat predation pressure (parameter estimate (PE) of bat abundance: 0.056, 95% confidence interval (CI): 0.015 – 0.056) (Fig. 3A). Seasonal temperature variation, average annual temperature, and average annual precipitation all had negative relationships with hindwing length, with seasonal temperature variation having the greatest effect size (PE seasonal temp variation: -0.062, CI: -0.10 to -0.020, PE temp: -0.047 CI: -0.071 to -0.023, PE precipitation: -0.027, CI: -0.047 to -0.007). Latitude, by contrast, did not appear to have a meaningful relationship with hindwing length (PE: 0.013, CI: -0.050 to 0.075) and growing season period had a positive association (PE: 0.033, CI: 0.014 to 0.052) (Fig. 3A). Comparing the global model with a null model (which only accounts for phylogenetic relationships), we found that while phylogenetic relationships alone explain much of the variance in hindwing length (log HW/Antenna length, $r^2 = 0.87$), the model with all parameters of interest explained more ($r^2 = 0.88$). Model fit of the full model was also better than the null (DIC full model: -539.5, DIC null model: -509.7; see Supplementary Materials). Moreover, removing bat diversity from the model decreased the explanatory power of the model by ~2% (r2_pred [70]; see code and outputs on Dryad). Breaking the dataset down by moth species also demonstrated that hindwing length was positively correlated with bat diversity in almost all species and was negatively correlated with seasonal temperature variation in almost all species (Fig. S10).

The pglmm analysis on forewing length (a proxy for body size [31,71]) showed a similar relationship with bat abundance (PE: 0.036, CI: 0.017 to 0.055), but fewer clear effects of environmental factors (PE precipitation: -0.029, CI: -0.048 to -0.010; PE temp: -0.025, CI: -0.047 to 0.002; PE seas temp: -0.022, CI: -0.060 to 0.016; PE latitude: -0.038, CI: -0.094 to 0.018). Here, only precipitation and temperature had a negative relationship with body size and

length of growing period had a positive relationship (PE LGP: 0.022, CI: 0.004 to 0.039) (Fig. 3B). Again, the model containing all parameters was a better fit than the null (DIC full model: -592.2, DIC null model: -574.0). Overall, however, the predictors explained less of the variance in body size (r^2=0.77) than hindwing length. From a set of interaction models, we found no significant interaction between bat abundance and seasonal temperature variation or length of growing period, indicating that the relationship between predation pressure and moth wing lengths are not being driven, or masked by, these environmental variables (see code and outputs in Dryad).

4. **Discussion**

Our macroevolutionary analysis provides evidence that bat predation pressure has exerted a strong selective force on the length of hindwing tails, while seasonal temperature variation has exerted a nearly equally counterbalancing constraint on hindwing length (Fig. 3A). Moths with long tails are therefore less likely to be found in areas with more temperature fluctuation across the year. This result is supported by the positive association between the length of growing period and hindwing tail length. In essence, areas with longer periods of high plant productivity and more consistent temperature regimes appear to be more permissive of the evolution of long hindwing tails than areas with more restrictive seasons. Although weaker than the seasonality parameters, we found a negative association between hindwing length and average annual temperature and precipitation, indicating an opposite trend from Allen's rule for endotherms, where appendages are expected to elongate in hotter, drier environments (as in [72]). This aligns with previous work indicating that Lepidoptera wings are not used for heat venting [73]. Despite the broadscale linkage between latitude and seasonality, we did not find an effect of latitude in

any of our models, indicating that the underlying drivers of wing trait evolution in this group are more complex than general latitudinal gradients. Additionally, while previous studies have found latitude to be an important correlate of bat diversity [74], others have found that it is not the most informative predictor, especially in the case of insectivores [75–77]. In congruence with this, we found relatively weak associations between insectivorous bat abundance and any of our climactic variables in the context of our global models (see code and outputs in Dryad). Thus, the effects of predators and environment on moth hindwing tails are not confounded in this study. We note that different bat species may exert differing predatory pressures on saturniid moths based on specifics of their echolocation strategy or feeding guild [78], but given the large-scale nature of our data set and the generally similar diets of these aerial insectivores, we have considered insectivorous bats as a pooled group for the purposes of this study. Together, our analyses indicate that tails are locked in evolutionary tension between abiotic constraints and biotic pressure.

Contrary to our predictions, body size (forewing length) demonstrated an almost identical positive association with bat abundance as hindwing length (Fig. 3B). This could be because wing/body sizes are tightly integrated such that long hindwing tails require, or are made possible by, larger body sizes. This does not seem to be a ubiquitous rule in saturniids, as previous work in the subfamily Arsenurinae found an inverse relationship between hindwing length and body size (using forewing length as a proxy) [31]. However, arsenurine tails have a different structure than those of the Saturniinae (the subfamily containing *Actias*), in that they often protrude off the distal hindwing veins, rather than proximate ones [79]. We therefore think it is quite likely that these two subfamilies have different relationships between body size and hindwing tail length. In our clade of interest hindwing length scales with forewing length ($R^2 = 0.60$; Fig. S6) and thus

most likely body size. Rather than simply being a necessary precursor for long hindwing tails, however, body size may be an anti-bat trait in itself. Bats seem to target prey relative to their own size, such that smaller bats eat smaller insects and larger bats are the main predators of large moths and beetles [80,81]. Whether this is due to handling, gape size, or echolocation limitations is still debated [44,82–84]. We found that the positive association between bat abundance and forewing length is complemented by a positive association between length of growing period and forewing length, again indicating that longer periods of forage availability allow for longer periods of larval feeding and larger adult body sizes [15]. These effects were to some extent countered by a negative association with precipitation. This may indicate a limitation on body size in regions with more rainfall, perhaps due to hampered foraging or increased larval mortality during bouts of heavy rain [85]. However, precipitation parameters from Worldclim should be considered with caution, especially from tropical regions with fewer climactic field data collection stations [86].

In addition to its use in our statistical models, comparative trait analyses on our dated and well-sampled *Actias* phylogeny revealed multiple origins of tail elongation but only one adaptive peak at the stem of the long-tailed moon moth clade, comprising all tailed species. This may be a result of the relatively limited number of species in this group and the strong phylogenetic signal underlying the tail trait. That is, while hindwing length varies considerably among these species, all species in this clade have tails, possibly making it more difficult to find the valleys between the morphological peaks [67,87]. Our results are congruent with a prior study that inferred a similar adaptive peak regime in *Argema* + *Actias* that was convergently repeated across the tree [11]. The multiple elongation events across our phylogeny indicates that the tail is a labile trait that could have become enhanced under conditions of high enough echolocating predator

pressure and permissive environmental conditions. Previous research into the morphological lability of the fore- and hindwings of tailed swallowtail butterflies (Papillionidae), found similarly elevated hindwing shape diversity [88]. Lepidopteran wing shape variation is likely driven by different biological pressures on the two sets of wings, where forewings are essential for flight, while hindwings are helpful for maneuverability, but not entirely necessary [89–91]. Further, experimental evidence indicates that rather than being purely flight-driven, hindwings can play an important role in deflecting predators both during the day [92] and night [10,11].

Based on our results and previous dated bat phylogenies, tailed moon moths were likely subject to bat predation throughout their evolutionary history. *Argema* + *Actias* diverged from their non-tailed sister taxa ~20 mya and *Argema* and *Actias* diverged ~15 mya, most likely in Africa. Based on fossil evidence [93,94] and biogeographical reconstructions [93,95–98], large insectivorous bats had already become globally spread by this time (~15 mya). Moreover, current dated bat phylogenies indicate that many extant lineages diversified 10-15 mya [94,99]. This rise in bat diversity and widespread prevalence of these predators could have made hindwing protrusions more profitable, as the night sky filled with more echolocators exploiting a greater depth of the prey community [100]. The three longest-tailed moth lineages within *Actias* all appear to have diverged ~7 mya and eventually moved to different parts of Asia: *Actias dubernardi* + *A. chapae* primarily in the East Palearctic, *Actias rhodopneuma* primarily in Malaysia and India, and *Actias isis* + *A. philippinica* + *A. maenas* primarily in the Indo-Australian archipelago (Indonesia, Philippines, Borneo). Lineages leading to *G. isabellae* and *Actias luna* + *truncatipennis* had slightly different trajectories, diverging from the rest of *Actias* ~9 mya and sometime later becoming established in Europe and North America, respectively (Fig. 1). Over the course of this time, the climate [101] and land masses were similar to current-

day conditions, aside from movements of the Indo-Australian archipelago that continued until ~5 mya [102] and the closure of the Bering bridge (which may have facilitated the movement of *Actias* to the North American continent) [103,104]. The relatively young age of this clade is therefore one of the strengths of this study. While there are risks to making assumptions about past predator and prey dynamics based on extant forms, interactions, or distributions [105], the relative consistency of environmental conditions and bat presence strengthens our inferential power. Additionally, while our bat abundance estimates come with necessary assumptions and levels of uncertainty (e.g., species distribution models of extant species can be uncertain for species that are difficult to "observe", as is the case with some insectivorous bats [106,107] and the population estimates were built from a global mammal dataset which likely provided coarse estimates [58]), we are ultimately interested in relative, rather than absolute, predator abundance. In general, species richness – the backbone upon which we built our abundance estimates – remains stable when ecological limits (most driven by climactic variables) are similar [108–110]. Thus, while extant bat distributions may not directly mirror historical ones, moths were clearly under intense selection pressure by echolocating bats in these regions.

In sum, results from this study, in conjunction with previous behavioral work [10,11] provide synergistic compelling evidence that predation pressure by bats has driven the elongation of hindwing tails in moon moths. Considering the absence of alternative selective forces (i.e., reproduction [13] or diurnal predation [14]) and the clear efficacy of even short tails to increase escape success [11], we postulate that bat predation pressure drove the origins of the hindwing tail in Saturniidae. Long hindwing tails have emerged five independent times across Saturniidae, three times in the Saturniinae (tribes: Saturniini, Attacini, Urotini/Bunaeini), once within the Arsenurinae [10,11,31], and once in Cercophaninae [19,111,112]. Phylogenetic inertia and the

seemingly easily modifiable unit of wing imaginal discs in developing Lepidoptera [113] likely played a role in the evolution of tails. Contrary to the tail-elongating force of predation pressure, the elaboration of this trait appears to be limited by environmental factors. While developmental studies are needed to uncover the mechanism by which environment constrains tail enhancement (i.e., building a tail may require more nutritional resources and a longer growing season than building a more simplified hindwing), the negative association that we found between climatic variables, and the positive association with longer growing periods, provides evidence for an environmentally-mediated long-term cost of these appendages. A similar relationship was previously found between bright butterfly coloration, climatic variables, and bird diversity, indicating that trait elaboration of multiple kinds is likely limited by environmental factors [114]. Interestingly, while these environmental parameters may restrict tail extension, it appears that shifts towards tail shrinkage are relatively uncommon (Fig. 1). Whether this is due to phylogenetic constraint, or due to the overwhelming benefit of having a tail versus lacking one requires further research. Here, our study adds an important macrovevolutionary lens to previous experimental predator-prey work. Uniting these two levels of information provides important advancement to our understanding of complex evolutionary dynamics and opens new lines of inquiry for future research [115]. Such multi-scale investigation into the relative pressures of competing eco-evolutionary forces can help illuminate the historical context within which other elaborate traits have originated and diversified across taxonomic systems.

References

1. Graham ZA, Garde E, Heide-Jørgensen MP, Palaoro A V. 2020 The longer the better: Evidence that narwhal tusks are sexually selected. *Biol Lett* **16**, 1–5. (doi:10.1098/rsbl.2019.0950)
2. Petrie M, Tim H, Carolyn S. 1991 Peahens prefer peacocks with elaborate trains. *Anim Behav* **41**, 323–331. (doi:10.1016/S0003-3472(05)80484-1)
3. Crofts SB, Stankowich T. 2021 Stabbing spines: A review of the biomechanics and evolution of defensive spines. *Integr Comp Biol* **61**, 655–667. (doi:10.1093/icb/icab099)
4. Garland T, Downs CJ, Ives AR. 2022 Trade-offs (And constraints) in organismal biology. *Physiological and Biochemical Zoology* **95**, 82–112. (doi:10.1086/717897)
5. Basolo AL, Alcaraz G. 2003 The turn of the sword: Length increases male swimming costs in swordtails. *Proceedings of the Royal Society B: Biological Sciences* **270**, 1631–1636. (doi:10.1098/rspb.2003.2388)
6. Somjee U. 2021 Positive allometry of sexually selected traits: Do metabolic maintenance costs play an important role? *BioEssays* **43**, 1–13. (doi:10.1002/bies.202000183)
7. Thavarajah NK, Tickle PG, Nudds RL, Codd JR. 2016 The peacock train does not handicap cursorial locomotor performance. *Sci Rep* **6**, 1–6. (doi:10.1038/srep36512)
8. Møller AP. 1996 The cost of secondary sexual characters and the evolution of cost-reducing traits. *Ibis* **138**, 112–119. (doi:10.1111/j.1474-919x.1996.tb04317.x)
9. Scoble MJ. 1992 *The Lepidoptera. Form, function and diversity*. Oxford: Oxford University Press.
10. Barber JR, Leavell BC, Keener AL, Breinholt JW, Chadwell BA, McClure CJW, Hill GM, Kawahara AY. 2015 Moth tails divert bat attack: Evolution of acoustic deflection. *Proceedings of the National Academy of Sciences* **112**, 2812–2816. (doi:10.1073/pnas.1421926112)
11. Rubin JJ, Hamilton CA, McClure CJW, Chadwell BA, Kawahara AY, Barber JR. 2018 The evolution of anti-bat sensory illusions in moths. *Sci Adv* **4**, 1–10. (doi:10.1126/sciadv.aar7428)
12. Procheş Ş. 2005 The world's biogeographical regions: Cluster analyses based on bat distributions. *J Biogeogr* **32**, 607–614. (doi:10.1111/j.1365-2699.2004.01186.x)
13. Rubin JJ, Kawahara AY. 2023 Sexual selection does not drive hindwing tail elaboration in a moon moth, Actias luna. *Behavioral Ecology* **34**, 488–494. (doi:10.1093/beheco/arad019)
14. Rubin JJ, Martin NW, Sieving KE, Kawahara AY. 2023 Testing bird-driven diurnal trade-offs of the moon moth's anti-bat tail. *Biol Lett* **19**, 1–5. (doi:10.1098/rsbl.2022.0428)
15. Nijhout HF, Riddiford LM, Mirth C, Shingleton AW, Suzuki Y, Callier V. 2014 The developmental control of size in insects. *Rev Dev Biol* **3**, 113–134. (doi:10.1002/wdev.124)
16. McKenna KZ, Tao D, Nijhout HF. 2019 Exploring the role of insulin signaling in relative growth: A case study on wing-body scaling in Lepidoptera. *Integr Comp Biol* **59**, 1324–1337. (doi:10.1093/icb/icz080)
17. Nijhout HF, Emlen DJ. 1998 Competition among body parts in the development and evolution of insect morphology. *PNAS* **95**, 3685–3689. (doi:10.1073/pnas.95.7.3685)
18. Macdonald WP, Martin A, Reed RD. 2010 Butterfly wings shaped by a molecular cookie cutter: Evolutionary radiation of lepidopteran wing shapes associated with a derived Cut/wingless wing margin boundary system. *Evol Dev* **12**, 296–304. (doi:10.1111/j.1525-142X.2010.00415.x)
19. Hamilton CA, St Laurent RA, Dexter K, Kitching IJ, Breinholt JW, Zwick A, Timmermans MJTN, Barber JR, Kawahara AY. 2019 Phylogenomics resolves major relationships and reveals significant diversification rate shifts in the evolution of silk moths and relatives. *BMC Evol Biol* **19**, 1–13. (doi:10.1186/s12862-019-1505-1)
20. Kawahara AY, Plotkin D, Espeland M, Meusemann K, Toussaint EFA. 2019 Phylogenomics reveals the evolutionary timing and pattern of butterflies and moths. *PNAS* , 1–7. (doi:10.1073/pnas.1907847116)
21. Tobler A, Nijhout HF. 2010 Developmental constraints on the evolution of wing-body allometry in *Manduca sexta*. *Evol Dev* **12**, 592–600. (doi:10.1111/j.1525-142X.2010.00444.x)
22. Mousseau TA. 1997 Ectotherms follow the converse to Bergmann's rule. **51**, 630–632. (doi:10.2307/2411138)
23. Dmitriew CM. 2011 The evolution of growth trajectories: What limits growth rate? *Biological Reviews* **86**, 97–116. (doi:10.1111/j.1469-185X.2010.00136.x)
24. Lehnert MS, Scriber JM, Gerard PD, Emmel TC. 2012 The 'converse to Bergmann's rule' in tiger swallowtail butterflies: boundaries of species and subspecies wing traits are independent of thermal and host-plant induction. *American Entomologist* **53**, 156–165.

25. Plaistow SJ, Tsuchida K, Tsubaki Y, Setsuda K. 2005 The effect of a seasonal time constraint on development time, body size, condition, and morph determination in the horned beetle *Allomyrina dichotoma* L. (Coleoptera: Scarabaeidae). *Ecol Entomol* **30**, 692–699. (doi:10.1111/j.0307-6946.2005.00740.x)
26. Beerli N, Bärtschi F, Ballesteros-Mejia L, Kitching IJ, Beck J. 2019 How has the environment shaped geographical patterns of insect body sizes? A test of hypotheses using sphingid moths. *J Biogeogr* **46**, 1687–1698. (doi:10.1111/jbi.13583)
27. Brehm G, Zeuss D, Colwell RK. 2019 Moth body size increases with elevation along a complete tropical elevational gradient for two hyperdiverse clades. *Ecography* **42**, 632–642. (doi:10.1111/ecog.03917)
28. Svensson EI, Gómez Llano M, Waller JT. 2022 Out of the tropics: Macroevolutionary size trends in an old insect order are shaped by temperature and predators. *J Biogeogr* , 1–14. (doi:10.1111/jbi.14544)
29. Shelomi M, Zeuss D. 2017 Bergmann's and Allen's rules in native European and Mediterranean Phasmatodea. *Front Ecol Evol* **5**, 1–13. (doi:10.3389/fevo.2017.00025)
30. D'Abrera B. 1995 *Saturniidae Mundi*. Antiquariat Goecke & Evers.
31. Hamilton CA, Winiger N, Rubin JJ, Breinholt J, Rougerie R, Kitching IJ, Barber JR, Kawahara AY. 2022 Hidden phylogenomic signal helps elucidate Arsenurine silkmoth phylogeny and the evolution of body size and wing shape trade-offs. *Syst Biol* **71**, 859–874. (doi:10.1093/sysbio/syab090)
32. Miller WE. 1977 Wing Measure as a size index in Lepidoptera: the family Olethreutidae. *Ann Entomol Soc Am* **70**, 253–256. (doi:10.1093/aesa/70.2.253)
33. Breinholt JW, Earl C, Lemmon AR, Moriarty Lemmon E, Xiao L, Kawahara AY. 2017 Resolving relationships among the megadiverse butterflies and moths with a novel pipeline for Anchored Phylogenomics. *Syst Biol* **0**, 1–16. (doi:10.1093/sysbio/syx048)
34. Larsson A. 2014 AliView: A fast and lightweight alignment viewer and editor for large datasets. *Bioinformatics* **30**, 3276–3278. (doi:10.1093/bioinformatics/btu531)
35. Kück P, Longo GC. 2014 FASconCAT-G: extensive functions for multiple sequence alignment preparations concerning phylogenetic studies. *Front Zool* **11**, 81. (doi:10.1186/s12983-014-0081-x)
36. Nguyen LT, Schmidt HA, Von Haeseler A, Minh BQ. 2015 IQ-TREE: A fast and effective stochastic algorithm for estimating maximum-likelihood phylogenies. *Mol Biol Evol* **32**, 268–274. (doi:10.1093/molbev/msu300)
37. Drummond AJ, Rambaut A. 2007 BEAST: Bayesian evolutionary analysis by sampling trees. *BMC Evol Biol* **7**. (doi:10.1186/1471-2148-7-214)
38. Lanfear R, Calcott B, Ho SYW, Guindon S. 2012 PartitionFinder: Combined selection of partitioning schemes and substitution models for phylogenetic analyses. *UPB Scientific Bulletin, Series B: Chemistry and Materials Science* **29**, 1695–1701. (doi:10.1093/molbev/mss020)
39. Mirarab S, Warnow T. 2015 ASTRAL-II: Coalescent-based species tree estimation with many hundreds of taxa and thousands of genes. *Bioinformatics* **31**, i44–i52. (doi:10.1093/bioinformatics/btv234)
40. Maddison W, Maddison D. 2022 Mesquite: A modular system for evolutionary analysis. Version 3.60. *http://www.mesquiteproject.org*.
41. Matzke N. 2018 BioGeoBEARS: BioGeography with Bayesian (and likelihood) evolutionary analysis with R Scripts. *R Package, Version 1.1.1*. **1**.
42. Toussaint EFA *et al.* 2019 Out of the Orient: Post-Tethyan transoceanic and trans-Arabian routes fostered the spread of Baorini skippers in the Afrotropics. *Syst Entomol* **44**, 926–938. (doi:10.1111/syen.12365)
43. Baker RJ, Bininda-Edmonds ORP, Mantilla-Meluk H, Porter CA, Van Den Bussche RA. 2012 Molecular time scale of diversification of feeding strategy and morphology in New World Leaf-Nosed Bats (Phyllostomidae): a phylogenetic perspective. In *Evolutionary history of bats: fossils, molecules, and morphology* (eds GF Gunnell, NB Simmons), pp. 385–409. New York: Cambridge University Press.
44. Barclay RMR, Brigham RM. 1991 Prey detection, dietary niche breadth, and body size in bats: why are aerial insectivorous bats so small? *Am Nat* **137**, 693–703. (doi:10.1080/0305006790150101)
45. Folk RA, Siniscalchi CM, Doby J, Kates HR, Manchester SR, Soltis PS, Soltis DE, Guralnick RP, Belitz M. 2023 Spatial phylogenetics of Fagales: Investigating the history of temperate forests. *BioRxiv* (doi:10.1101/2023.04.17.537249)
46. Abbott JC, Bota-Sierra CA, Guralnick R, Kalkman V, González-Soriano E, Novelo-Gutiérrez R, Bybee S, Ware J, Belitz MW. 2022 Diversity of nearctic dragonflies and damselflies (Odonata). *Diversity* **14**, 1–18. (doi:10.3390/d14070575)
47. Simmons NB, Cirranello AL. In press. Bat species of the world: A taxonomic and geographic database, version 1.3. *2022*.

48. Zizka A *et al.* 2019 CoordinateCleaner: Standardized cleaning of occurrence records from biological collection databases. *Methods Ecol Evol* **10**, 744–751. (doi:10.1111/2041-210X.13152)
49. Herkt KMB, Barnikel G, Skidmore AK, Fahr J. 2016 A high-resolution model of bat diversity and endemism for continental Africa. *Ecol Modell* **320**, 9–28. (doi:10.1016/j.ecolmodel.2015.09.009)
50. Smeraldo S *et al.* 2018 Ignoring seasonal changes in the ecological niche of non-migratory species may lead to biases in potential distribution models: lessons from bats. *Biodivers Conserv* **27**, 2425–2441. (doi:10.1007/s10531-018-1545-7)
51. Hayes MA, Cryan PM, Wunder MB. 2015 Seasonally-dynamic presence-only species distribution models for a cryptic migratory bat impacted by wind energy development. *PLoS One* **10**. (doi:10.1371/journal.pone.0132599)
52. McClure ML *et al.* 2021 A hybrid correlative-mechanistic approach for modeling winter distributions of North American bat species. *J Biogeogr* **48**, 2429–2444. (doi:10.1111/jbi.14130)
53. Fick SE, Hijmans RJ. 2017 WorldClim 2: new 1-km spatial resolution climate surfaces for global land areas. *International Journal of Climatology* **37**, 4302–4315. (doi:10.1002/joc.5086)
54. Amatulli G, Domisch S, Tuanmu M-N, Parmentier B, Ranipeta A, Malczyk J, Jetz W. 2018 A suite of global, cross-scale topographic variables for environmental and biodiversity modeling. *Sci Data* **5**, 1–15. (doi:10.1038/sdata.2018.40)
55. Townsend J, DiMiceli C. 2015 MOD44B MODIS/Terra Vegetation Continuous Fields Yearly L3 Global 500m SIN Grid. *NASA LP DAAC*.
56. Kass JM *et al.* 2022 The global distribution of known and undiscovered ant biodiversity. *Sci. Adv*. **8**.
57. Calabrese JM, Certain G, Kraan C, Dormann CF. 2014 Stacking species distribution models and adjusting bias by linking them to macroecological models. *Global Ecology and Biogeography* **23**, 99–112. (doi:10.1111/geb.12102)
58. Greenspoon L *et al.* 2023 The global biomass of wild mammals. *PNAS* **120**. (doi:10.1073/pnas.2204892120)
59. Chamberlain S, Barve V, Mcglinn D, Oldoni D, Desmet P, Geffert L, Ram K. 2023 rgbif: Interface to the Global Biodiversity Information Facility API. *R package version 3.3.7*.
60. Rasband WS. 2018 ImageJ.
61. Acharya L. 1995 Sex-biased predation on moths by insectivorous bats. *Anim Behav* **49**, 1461–1468. (doi:10.1016/0003-3472(95)90067-5)
62. Li D, Dinnage R, Nell LA, Helmus MR, Ives AR. 2020 phyr: An r package for phylogenetic species-distribution modelling in ecological communities. *Methods Ecol Evol* **11**, 1455–1463. (doi:10.1111/2041-210X.13471)
63. Fischer G, van Velthuizen H, Nachtergaele FO. 2000 Global Agro-Ecological Zones Assessment: Methodology and Results.
64. Zuur AF, Ieno EN, Elphick CS. 2010 A protocol for data exploration to avoid common statistical problems. *Methods Ecol Evol* **1**, 3–14. (doi:10.1111/j.2041-210x.2009.00001.x)
65. Revell LJ. 2012 phytools: An R package for phylogenetic comparative biology (and other things). *Methods Ecol Evol* **3**, 217–223. (doi:10.1111/j.2041-210X.2011.00169.x)
66. Goolsby EW, Bruggeman J, Ané C. 2017 Rphylopars: fast multivariate phylogenetic comparative methods for missing data and within-species variation. *Methods Ecol Evol* **8**, 22–27. (doi:10.1111/2041-210X.12612)
67. Ingram T, Mahler DL. 2013 SURFACE: Detecting convergent evolution from comparative data by fitting Ornstein-Uhlenbeck models with stepwise Akaike Information Criterion. *Methods Ecol Evol* **4**, 416–425. (doi:10.1111/2041-210X.12034)
68. Nässig WA. 1991 Biological observations and taxonomic notes on *Actias isabellae* (Graells) (Lepidoptera, Saturniidae). *Nota lepidoptera* **14**, 131–143.
69. Ylla J, Peigler RS, Kawahara AY. 2005 Cladistic analysis of moon moths using morphology, molecules, and behaviour: *Actias* Leach, 1815; *Argema* Wallengren, 1858; *Graellsia* Grote, 1896 (Lepidoptera: Saturniidae). *SHILAP Revista de Lepidoterologia* **33**, 299–317.
70. Ives AR. 2019 R2s for Correlated Data: Phylogenetic Models, LMMs, and GLMMs. *Syst Biol* **68**, 234–251. (doi:10.1093/sysbio/syy060)
71. Miller WE. 1997 Diversity and evolution of tongue length in hawkmoths (Sphingidae). *J Lepid Soc* **51**, 9–31.
72. Alhajeri BH, Fourcade Y, Upham NS, Alhaddad H. 2020 A global test of Allen's rule in rodents. *Global Ecology and Biogeography* **29**, 2248–2260. (doi:10.1111/geb.13198)
73. Wasserthal LT. 1975 The role of butterfly wings in regulation of body temperature. *J Insect Physiol* **21**, 1921–1930. (doi:10.1016/0022-1910(75)90224-3)

74. Kaufman DM, Willig MR. 1998 Latitudinal patterns of mammalian species richness in the New World: The effects of sampling method and faunal group. *J Biogeogr* **25**, 795–805. (doi:10.1046/j.1365-2699.1998.2540795.x)
75. Martins MA, Carvalho WD De, Dias D, Franca DDS, Oliveira MBD, Peracchi AL. 2015 Bat species richness (Mammalia, Chiroptera) along an elevational gradient in the Atlantic forest of southeastern Brazil. *Acta Chiropt* **17**, 401–409. (doi:10.3161/15081109ACC2015.17.2.016)
76. Bogoni JA, Carvalho-Rocha V, Ferraz KMPMB, Peres CA. 2021 Interacting elevational and latitudinal gradients determine bat diversity and distribution across the Neotropics. *Journal of Animal Ecology*. (doi:10.1111/1365-2656.13594)
77. Patten MA. 2004 Correlates of species richness in North American bat families. *J Biogeogr* **31**, 975–985. (doi:10.1111/j.1365-2699.2004.01087.x)
78. Denzinger A, Schnitzler HU. 2013 Bat guilds, a concept to classify the highly diverse foraging and echolocation behaviors of microchiropteran bats. *Front Physiol* **4**, 1–15. (doi:10.3389/fphys.2013.00164)
79. Zhong M, Hilla GM, Gomez JP, Plotkin D, Barber JR, Kawahara AY. 2016 Quantifying wing shape and size of saturniid moths with geometric morphometrics. *J Lepid Soc* **70**, 99–107. (doi:10.18473/lepi.70i2.a4)
80. Wray AK, Peery MZ, Jusino MA, Kochanski JM, Banik MT, Palmer JM, Lindner DL, Gratton C. 2021 Predator preferences shape the diets of arthropodivorous bats more than quantitative local prey abundance. *Mol Ecol* **30**, 855–873. (doi:10.1111/mec.15769)
81. Jones G. 1990 Prey selection by the greater horseshoe bat (*Rhinolophus* ferrumequinum): Optimal foraging by echolocation? *Journal of Animal Ecology* **59**, 587–602.
82. Gonsalves L, Bicknell B, Law B, Webb C, Monamy V. 2013 Mosquito consumption by insectivorous bats: Does size matter? *PLoS One* **8**. (doi:10.1371/journal.pone.0077183)
83. Giacomini G, Herrel A, Chaverri G, Brown RP, Russo D, Scaravelli D, Meloro C. 2022 Functional correlates of skull shape in Chiroptera: feeding and echolocation adaptations. *Integr Zool* **17**, 430–442. (doi:10.1111/1749-4877.12564)
84. Bogdanowicz W, Fenton MB, Daleszczyk K. 1999 The relationships between echolocation calls, morphology and diet in insectivorous bats. *J Zool* **247**, 381–393. (doi:10.1111/j.1469-7998.1999.tb01001.x)
85. Kamata N, Igarashi Y. 1994 Influence of rainfall on feeding behavior, growth, and mortality of larvae of the beech caterpillar, *Quadricalcarifera punctatella* (Motschulsky) (Lep., Notodontidae). *Journal of Applied Entomology* **118**, 347–353. (doi:10.1111/j.1439-0418.1994.tb00810.x)
86. Soria-Auza RW, Kessler M, Bach K, Barajas-Barbosa PM, Lehnert M, Herzog SK, Böhner J. 2010 Impact of the quality of climate models for modelling species occurrences in countries with poor climatic documentation: a case study from Bolivia. *Ecol Modell* **221**, 1221–1229. (doi:10.1016/j.ecolmodel.2010.01.004)
87. Graham CH, Storch D, Machac A. 2018 Phylogenetic scale in ecology and evolution. *Global Ecology and Biogeography* **27**, 175–187. (doi:10.1111/geb.12686)
88. Owens HL, Lewis DS, Condamine FL, Kawahara AY, Guralnick RP. 2020 Comparative phylogenetics of *Papilio* butterfly wing shape and size demonstrates independent hindwing and forewing evolution. *Syst Biol* **69**, 813–819. (doi:10.1093/sysbio/syaa029)
89. Jantzen B, Eisner T. 2008 Hindwings are unnecessary for flight but essential for execution of normal evasive flight in Lepidoptera. *PNAS* **105**, 16636–40. (doi:10.1073/pnas.0807223105)
90. Stylman M, Penz CM, DeVries P. 2020 Large hind wings enhance gliding performance in ground effect in a Neotropical butterfly (Lepidoptera: Nymphalidae). *Ann Entomol Soc Am* **113**, 15–22. (doi:10.1093/aesa/saz042)
91. Le Roy C, Cornette R, Llaurens V, Debat V. 2019 Effects of natural wing damage on flight performance in *Morpho* butterflies: what can it tell us about wing shape evolution? *Journal of Experimental Biology* **222**, 1–10. (doi:10.1242/jeb.204057)
92. Chotard A, Ledamoisel J, Decamps T, Herrel A, Chaine AS, Llaurens V, Debat V. 2022 Evidence of attack deflection suggests adaptive evolution of wing tails in butterflies. *Proceedings of the Royal Society B: Biological Sciences* **289**. (doi:10.1098/rspb.2022.0562)
93. Teeling EC, Springer MS, Madsen O, Bates P, O'brien SJ, Murphy WJ. 2005 A molecular phylogeny for bats illuminates biogeography and the fossil record. *Science* **307**, 580–584. (doi:10.1126/science.1105113)
94. Shi JJ, Rabosky DL. 2015 Speciation dynamics during the global radiation of extant bats. *Evolution* **69**, 1528–1545. (doi:10.1111/evo.12681)

95. Ruedi M, Friedli-Weyeneth N, Teeling EC, Puechmaille SJ, Goodman SM. 2012 Biogeography of Old World emballonurine bats (Chiroptera: Emballonuridae) inferred with mitochondrial and nuclear DNA. *Mol Phylogenet Evol* **64**, 204–211. (doi:10.1016/j.ympev.2012.03.019)
96. Lamb JM *et al.* 2008 Phylogeography and predicted distribution of African-Arabian and Malagasy populations of giant mastiff bats, *Otomops* spp. (Chiroptera: Molossidae). *Acta Chiropt* **10**, 21–40. (doi:10.3161/150811008X331063)
97. HoráČek I, Fejfar O, Hulva P. 2006 A new genus of vespertilionid bat from Early Miocene of Jebel Zelten, Libya, with comments on *Scotophilus* and early history of vespertilionid bats (Chiroptera). *Lynx* **37**, 131–150.
98. Chornelia A, Hughes AC. 2022 The evolutionary history and ancestral biogeographic range estimation of old-world Rhinolophidae and Hipposideridae (Chiroptera). *BMC Ecol Evol* **22**. (doi:10.1186/s12862-022-02066-x)
99. Upham NS, Esselstyn JA, Jetz W. 2019 Inferring the mammal tree: Species-level sets of phylogenies for questions in ecology, evolution, and conservation. *PLoS Biol* **17**, e3000494. (doi:10.1371/journal.pbio.3000494)
100. Alberdi A *et al.* 2020 DNA metabarcoding and spatial modelling link diet diversification with distribution homogeneity in European bats. *Nat Commun* **11**, 1–8. (doi:10.1038/s41467-020-14961-2)
101. Steinthorsdottir M *et al.* 2021 The Miocene: The future of the past. *Paleoceanogr Paleoclimatol* **36**, 1–71. (doi:10.1029/2020PA004037)
102. Lohman DJ, De Bruyn M, Page T, Von Rintelen K, Hall R, Ng PKL, Shih H Te, Carvalho GC, Von Rintelen T. 2011 Beyond Wallaces line: Genes and biology inform historical biogeographical insights in the Indo-Australian archipelago. *Annu Rev Ecol Evol Syst* **42**. (doi:10.1146/annurev-ecolsys-102710-145001)
103. Hundsdoerfer AK, Kitching IJ, Wink M. 2005 A molecular phylogeny of the hawkmoth genus *Hyles* (Lepidoptera: Sphingidae, Macroglossinae). *Mol Phylogenet Evol* **35**, 442–458. (doi:10.1016/j.ympev.2005.02.004)
104. Rubinoff D, Doorenweerd C. 2020 Systematics and biogeography reciprocally illuminate taxonomic revisions in the silkmoth genus *Saturnia* (Lepidoptera: Saturniidae). *J Lepid Soc* **74**, 1–6. (doi:10.18473/lepi.74i1.a1)
105. Losos JB. 2011 Convergence, adaptation, and constraint. *Evolution* **65**, 1827–1840. (doi:10.1111/j.1558-5646.2011.01289.x)
106. Razgour O, Rebelo H, Di Febbraro M, Russo D. 2016 Painting maps with bats: species distribution modelling in bat research and conservation. *Hystrix* **27**, 1–8. (doi:10.4404/hystrix-27.1-11753)
107. Delgado-Jaramillo M, Aguiar LMS, Machado RB, Bernard E. 2020 Assessing the distribution of a species-rich group in a continental-sized megadiverse country: Bats in Brazil. *Divers Distrib* **26**, 632–643. (doi:10.1111/ddi.13043)
108. Rabosky DL, Hurlbert AH. 2015 Species richness at continental scales is dominated by ecological limits. *American Naturalist* **185**, 572–583. (doi:10.1086/680850)
109. Hawkins BA *et al.* 2012 Different evolutionary histories underlie congruent species richness gradients of birds and mammals. *J Biogeogr* **39**, 825–841. (doi:10.1111/j.1365-2699.2011.02655.x)
110. Dornelas M, Gotelli NJ, McGill B, Shimadzu H, Moyes F, Sievers C, Magurran AE. 2014 Assemblage time series reveal biodiversity change but not systematic loss. *Science* **344**, 296–299. (doi:10.1126/science.1248484)
111. Wolfe KL, Balcázar-Lara MA. 1994 Chile's *Cercophana venusta* and its immature stages (Lepidoptera: Cercophanidae). *Tropical Lepdioptera* **5**, 35–42.
112. Aiello BR *et al.* 2021 Adaptive shifts underlie the divergence in wing morphology in bombycoid moths. *Proc B* **288**, 20210677. (doi:10.1098/rspb.2021.0677)
113. Fisher CR, Wegrzyn JL, Jockusch EL. 2020 Co-option of wing-patterning genes underlies the evolution of the treehopper helmet. *Nat Ecol Evol* **4**, 250–260. (doi:10.1038/s41559-019-1054-4)
114. Dalrymple RL, Flores-Moreno H, Kemp DJ, White TE, Laffan SW, Hemmings FA, Hitchcock TD, Moles AT. 2018 Abiotic and biotic predictors of macroecological patterns in bird and butterfly coloration. *Ecol Monogr* **88**, 204–224. (doi:10.1002/ecm.1287)
115. McCleery R *et al.* 2023 Uniting experiments and big data to advance ecology and conservation. *Trends Ecol Evol* , 1–10. (doi:10.1016/j.tree.2023.05.010)

Data and materials availability: All data, code, and appendix materials will be made available at the Dryad Digital Repository (www.datadryad.org/xxxx) and Zenodo (www.zenodo.org/xxxx) upon acceptance.

Acknowledgments

Our sincere gratitude goes to Emily Ellis, who guided JJR in bioinformatics. David Plotkin helped with trouble-shooting phylogenetic and BioGeoBEARS analyses. Christian Couch and Amanda Markee contributed to DNA extraction and sequencing. Hailey Dansby helped collect photos of museum specimens. We appreciate David Grimaldi and Suzanne Green for help with AMNH specimen photos, as well as Stefan Naumann for providing *Actias felicis* photos and data. Sequenced specimens were collected with the help of several researchers, including Wayne Hsu, Charlie Mitter, and Richard Peigler. We thank José Miguel Ponciano for encouraging JJR to explore simulations at the start of this project, Emma Podietz for her help with ArcGIS, and Michael Belitz for his support on species richness estimation.

Funding

We thank the National Science Foundation for supporting this work: NSF DEB 1557007**,** NSF IOS 1920895, 1920936. JJR was supported by the UF Biology Graduate Student Fellowship and the SSB GIAR, CJC was supported by a UF Biodiversity Institute Fellowship and a Threadgill Dissertation Fellowship.

Figures

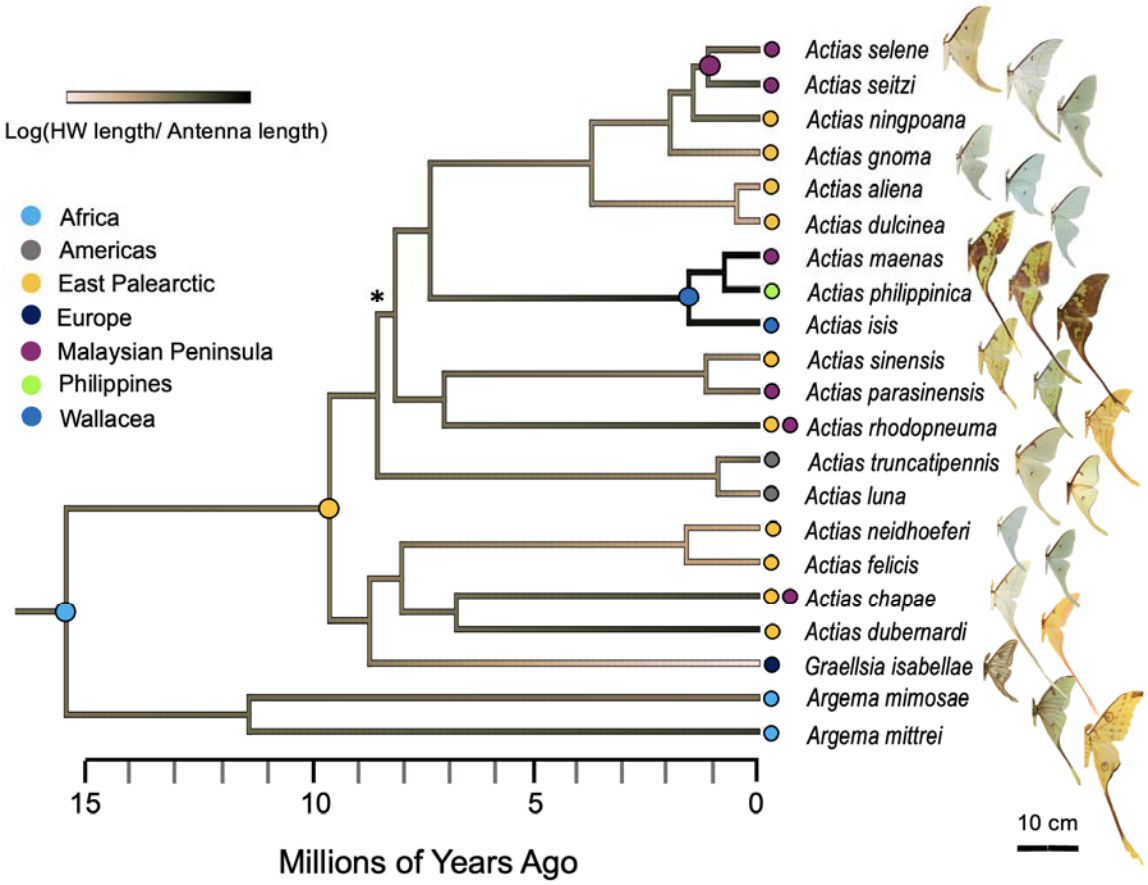

Figure 1. A time-calibrated tree of tailed moon moths (*Actias* + *Argema*) showing the inferred evolutionary and biogeographic history of long tails. Branches are colored by relative hindwing length (log(HW length/Antenna length)), with darker colors representing longer relative hindwing length. Median ages (in millions of years) were derived from a BEAST tree built with a Birth-Death prior using nodal calibrations from Kawahara et al. [20]. All support values from the starting maximum likelihood tree were 100/100, except at the node indicated by the asterisk, which was 80/100 (SH-aLRT). Colored circles represent results from our biogeographical (BioGeoBEARS) analysis, where the range remains the same as the ancestral node until there is a color shift.

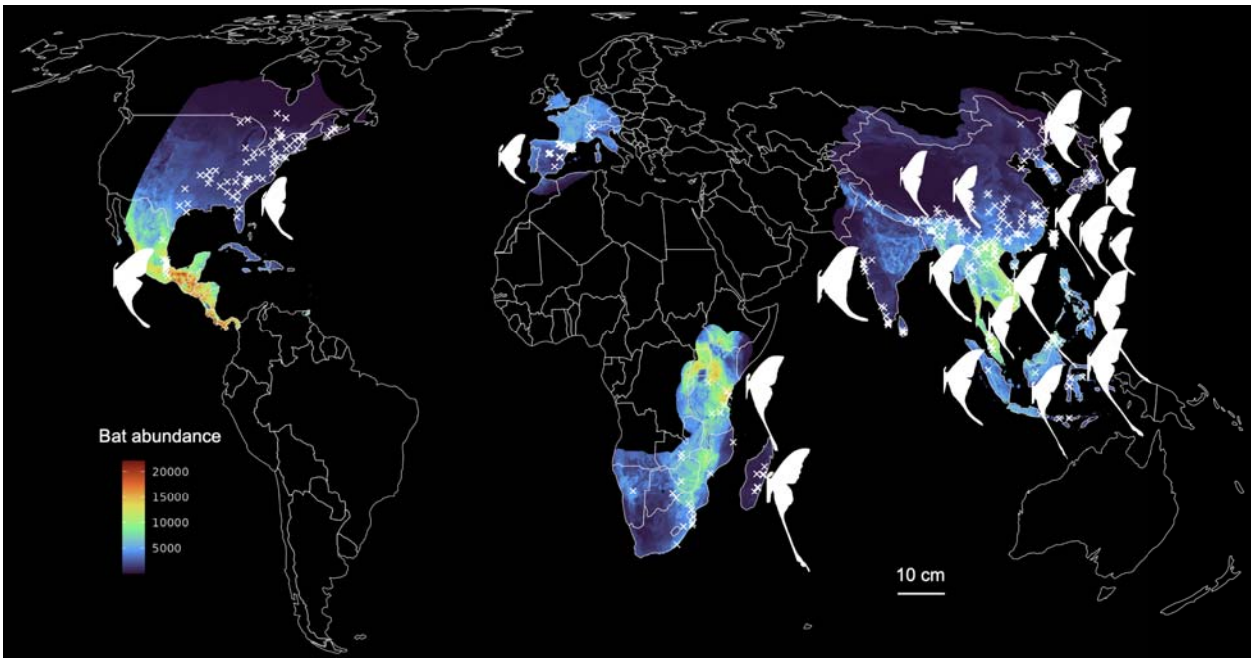

Figure 2. World map, pseudo-colored by bat predation pressure (sufficiently large, insectivorous bat abundance). We limited the visualization of our spatially explicit bat abundance estimates to only those areas that overlap with moth species of interest. Moth half-silhouettes indicate the general region where the species occurs. White x marks indicate precise moth observation locations, taken from museum collections, GBIF and iNaturalist. We extracted environmental variable values from WorldClim and length of growing season values from the UN FAO FGGD LGP map for each moth point. We used these parameters, as well as measurements from the associated moth photo and estimates of bat abundance at each point, to build our phylogenetically-informed models.

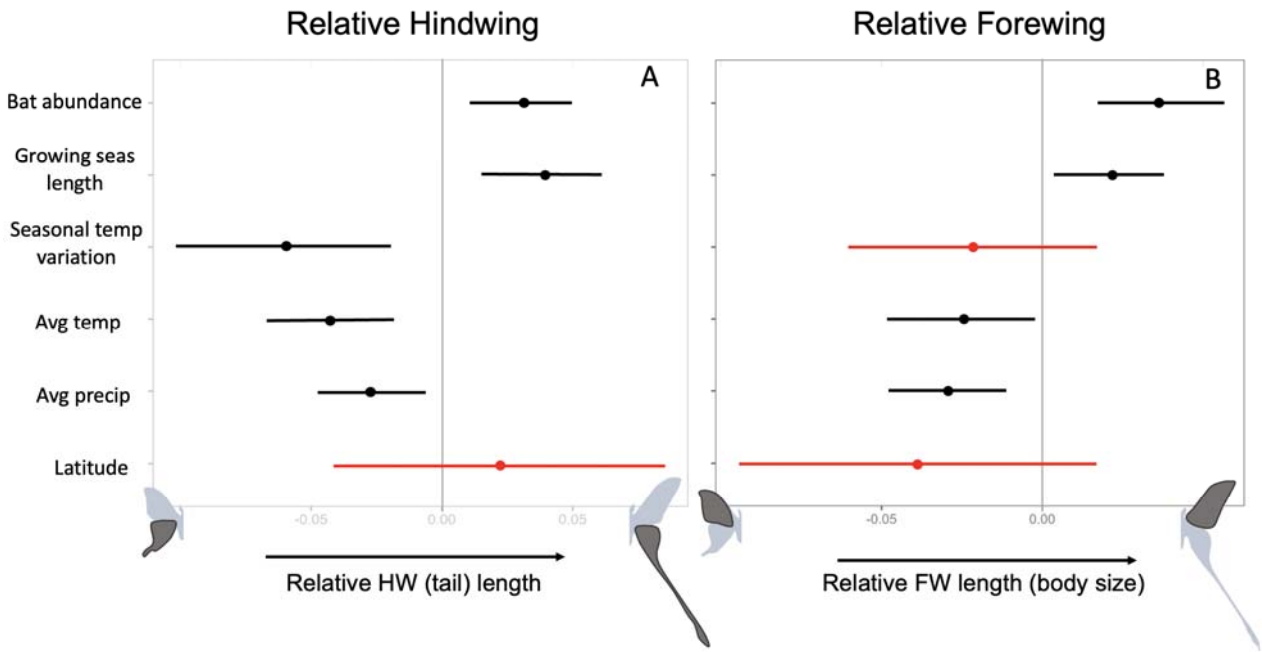

Figure 3. Tail length and body size (FW length) in the tailed moon moth group are driven by bats and constrained by environmental factors. Insectivorous bat abundance is positively correlated with A) hindwing and B) body size in the long-tailed moon moth clade. Seasonality (standard deviation of temperature across the year), average annual temperature and precipitation are negatively associated with hindwing length, while latitude overlaps the zero-line and is therefore an uninformative predictor. Growing season length is positively associated with both wing length traits, indicating that longer periods of plant productivity permit both the elongation of hindwing tails and the enlargement of body size (using forewing length as a proxy). Environmental constraints on forewing length were average temperature and precipitation. Central tendency dots indicate parameter estimates and error bars are 95% confidence intervals from the best fit phylogenetically-informed linear regression analyses. Red lines depict a parameter confidence interval overlapping zero. All predictor variables were mean center-scaled to make them comparable across units. Relative hindwing and forewing lengths are log(wing length/antenna length).